Supplementary Figures S1–S6

The clinical relevance of apocrine morphology in breast cancer depends on the estrogen receptor status

Kei Kawashima MD1,2, Masanori Oshi MD, PhD2, Akimitsu Yamada MD, PhD2, Kazutaka Narui MD, PhD3, Zunairah Shah MD, Thaer Khoury MD, Itaru Endo MD, PhD2, Kazuaki Takabe, MD, PhD, FACS, FSSO1,2,8,9,10,11

1 Department of Surgical Oncology, Roswell Park Comprehensive Cancer Center, Buffalo, NY 14263, USA
2 Department of Gastroenterological Surgery, Yokohama City University Graduate School of Medicine, Kanagawa, 236-0004, Japan
3 Department of Breast and Thyroid Surgery, Yokohama City University Medical Center, 4-57 Urafune-cho, Minami-ku, Yokohama City, Kanagawa, 232-0024, Japan.
8 Department of Surgery, University at Buffalo Jacobs School of Medicine and Biomedical Sciences, the State University of New York, Buffalo, NY, USA
9 Division of Digestive and General Surgery, Niigata University Graduate School of Medical and Dental Sciences, Niigata, Japan
10 Department of Breast Surgery and Oncology, Tokyo Medical University, Tokyo, Japan
11 Department of Breast Surgery, Fukushima Medical University, Fukushima, Japan

Supplementary figure S1

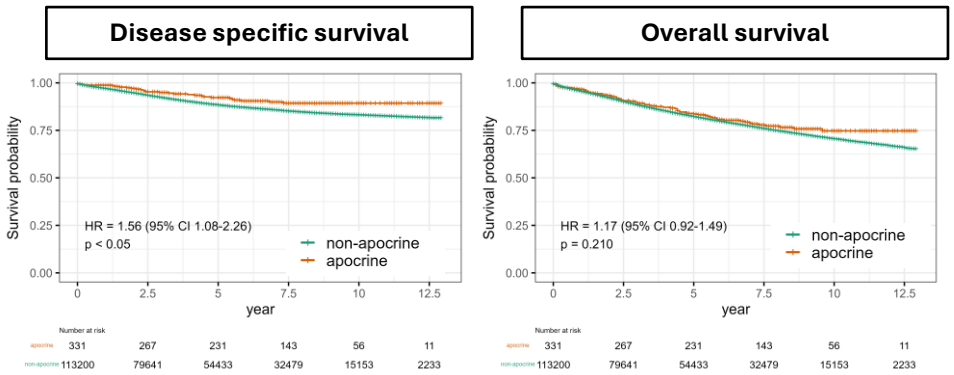

Supplementary figure S1: Analyses in the HER2-positive tumors. The analyses performed in the main text were also conducted in the HER2-positive subgroup. (A) Prognostic impact of apocrine carcinoma compared with non-apocrine carcinoma in the SEER cohort. Kaplan-Meier survival curves of disease-specific survival (DSS) and overall survival (OS) comparing apocrine and non-apocrine carcinomas in HER2-positive patients from the SEER cohort. Orange line represents apocrine carcinoma, and green line represents non-apocrine carcinoma. Hazard ratios (HRs) with 95% confidence intervals (CIs) were estimated using Cox proportional hazards models, and log-rank test P values are shown. Numbers at risk are displayed below each plot.

Supplementary figure S2

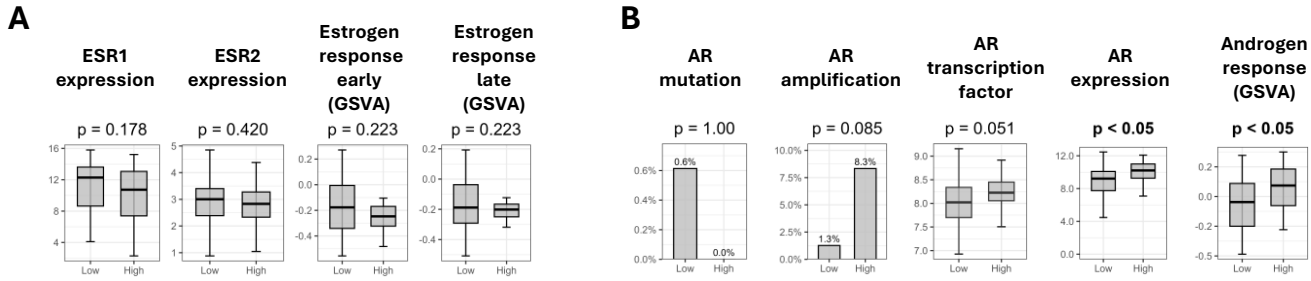

Supplementary Figure S2. Association of apocrine morphology with estrogen- and androgen-related features, and molecular subtypes in the TCGA cohort. (A) Box plots showing ESR1 and ESR2 expression levels, GSVA scores for the MSigDB Hallmark estrogen response early/late and androgen response gene set, stratified by apocrine morphology-high and -low group within HER2-positive breast cancers.. (B) Bar plots of AR mutation frequency and AR amplification frequency, and box plots of inferred AR transcription factor activity, AR gene expression level and GSVA scores for the MSigDB Hallmark androgen response gene set, stratified by apocrine morphology-high and -low group within HER2-positive breast cancers. In all boxplots, the center line indicates the median, the box represents the interquartile range (IQR), and whiskers extend to 1.5×IQR. Outliers were omitted. P values were calculated using the Wilcoxon rank-sum test.

Supplementary figure S3

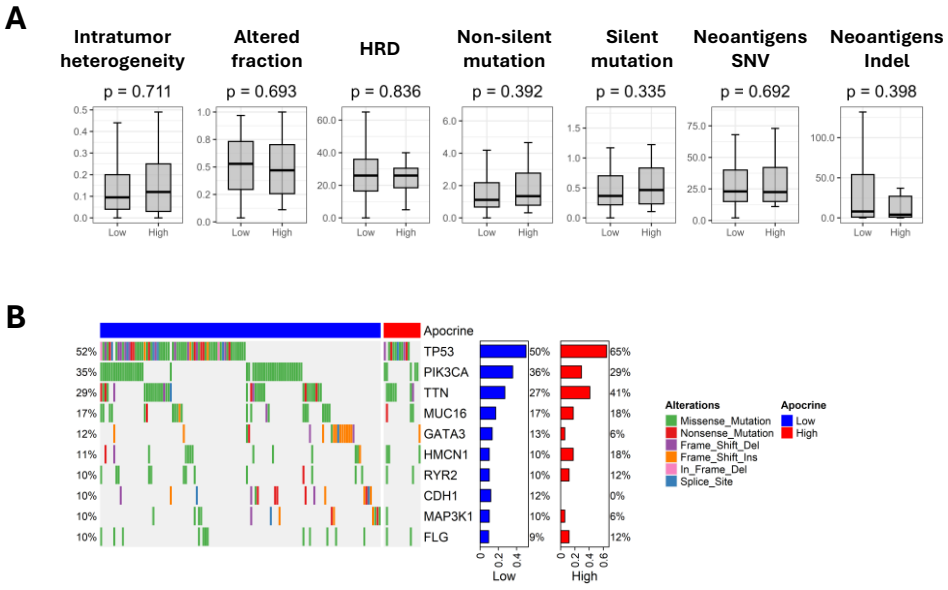

Supplementary Figure S3. Association of apocrine morphology with tumor immunogenicity-related scores and mutational landscapes. (A) Box plots showing intratumor heterogeneity, altered fraction, homologous recombination deficiency (HRD) score, non-silent and silent mutation burdens, and neoantigen load (SNV- and indel-derived) stratified by apocrine morphology across subtypes. (B) Oncoplot depicting recurrent somatic alterations in HER2-positive tumors, stratified by apocrine morphology. Alteration frequencies are shown on the right of each panel.

Supplementary figure S4

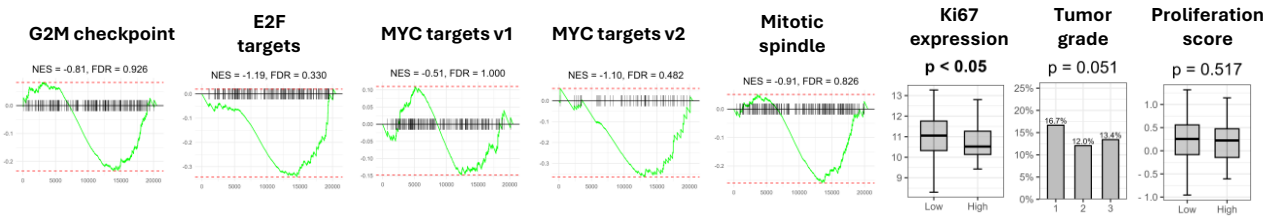

Supplementary Figure S4. Association of apocrine morphology with proliferative activity. Gene set enrichment analysis (GSEA) enrichment plots for proliferation-related MSigDB Hallmark pathways (G2M checkpoint, E2F targets, MYC targets v1/v2). Normalized enrichment score (NES) and false discovery rate (FDR) are shown for each pathway. Box plots comparing Ki-67 expression between apocrine-high and -low tumors, bar plots showing distribution of apocrine-high tumor across tumor grade, and box plots comparing proliferation score between apocrine-high and -low. P values were calculated using the Wilcoxon test.

Supplementary figure S5

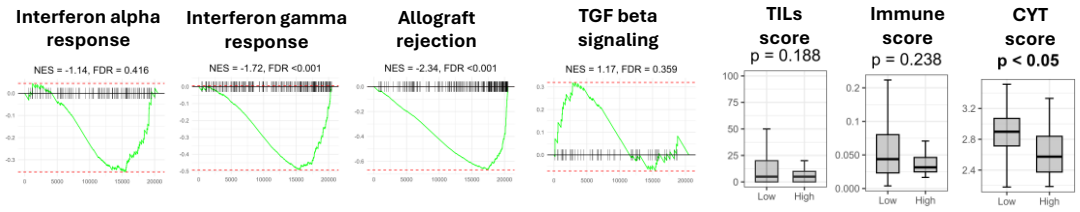

Supplementary Figure S5. Association of apocrine morphology with immune-related activity and immune-associated scores. Gene set enrichment analysis (GSEA) enrichment plots for immune-related Hallmark gene sets (interferon alpha signaling, interferon gamma signaling, allograft rejection, and TGF-β signaling) comparing apocrine-high and apocrine-low. Normalized enrichment score (NES) and false discovery rate (FDR) are shown for each pathway. Box plots showing tumor-infiltrating lymphocyte (TIL) score, immune score, and cytolytic activity (CYT) score stratified by apocrine morphology-high and -low group. P values for box plots were calculated using the Wilcoxon test.

Supplementary figure S6

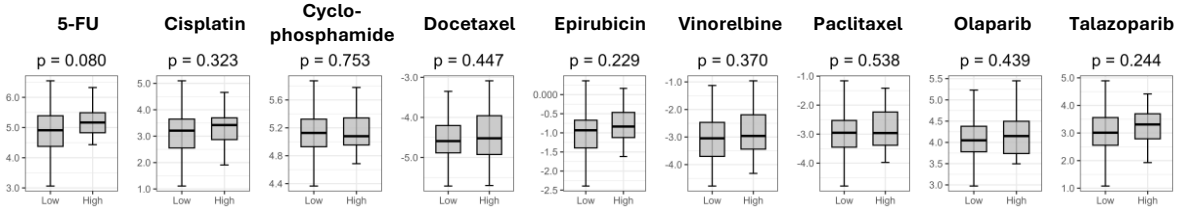

Supplementary Figure S6. Association of apocrine morphology with predicted response to anticancer therapeutics. Box plots comparing predicted drug response scores for standard chemotherapeutic agents and targeted therapies between apocrine-marked and apocrine-negative. Lower values reflect greater predicted sensitivity to the corresponding agent. P values were calculated using the Wilcoxon test.

Supplementary figure 2: Analyses in the HER2-positive tumors. The analyses performed in the main text were also conducted in the HER2-positive subgroup. (A) Prognostic impact of apocrine carcinoma compared with non-apocrine carcinoma in the SEER cohort. Kaplan-Meier survival curves of disease-specific survival (DSS) and overall survival (OS) comparing apocrine and non-apocrine carcinomas in HER2-positive patients from the SEER cohort. Orange line represents apocrine carcinoma, and green line represents non-apocrine carcinoma. Hazard ratios (HRs) with 95% confidence intervals (CIs) were estimated using Cox proportional hazards models, and log-rank test P values are shown. Numbers at risk are displayed below each plot. **(B) Association of apocrine morphology with estrogen- and androgen-related features, and molecular subtypes in the TCGA cohort.** Box plots showing ESR1 and ESR2 expression levels, GSVA scores for the MSigDB Hallmark estrogen response early/late and androgen response gene set, inferred AR transcription factor activity, and AR gene expression level stratified by apocrine morphology-high and -low group within HER2-positive breast cancers. In all boxplots, the center line indicates the median, the box represents the interquartile range (IQR), and whiskers extend to 1.5×IQR. Outliers were omitted. P values were calculated using the Wilcoxon rank-sum test. **(C) Association of apocrine morphology with tumor immunogenicity-related scores and mutational landscapes.** Box plots showing intratumor heterogeneity, altered fraction, homologous recombination deficiency (HRD) score, non-silent and silent mutation burdens, and neoantigen load (SNV- and indel-derived) stratified by apocrine morphology across subtypes. Oncoprints depicting recurrent somatic alterations in HER2-positive tumors, stratified by apocrine morphology. Alteration frequencies are shown on the right of each panel. **(D) Association of apocrine morphology with proliferative activity.** Gene set enrichment analysis (GSEA) enrichment plots for proliferation-related MSigDB Hallmark pathways (G2M checkpoint, E2F targets, MYC targets v1/v2). Normalized enrichment score (NES) and false discovery rate (FDR) are shown for each pathway. Box plots comparing Ki-67 expression between apocrine-high and -low tumors, bar plots showing distribution of apocrine-high tumor across tumor grade, and box plots comparing proliferation score between apocrine-high and -low. P values were calculated using the Wilcoxon test. **(E) Association of apocrine morphology with immune-related activity and immune-associated scores.** Gene set enrichment analysis (GSEA) enrichment plots for immune-related Hallmark gene sets (interferon alpha signaling, interferon gamma signaling, allograft rejection, and TGF-β signaling) comparing apocrine-high and apocrine-low. Normalized enrichment score (NES) and false discovery rate (FDR) are shown for each pathway. Box plots showing tumor-infiltrating lymphocyte (TIL) score, immune score, and cytolytic activity (CYT) score stratified by apocrine morphology-high and -low group. P values for box plots were calculated using the Wilcoxon test. **(F) Association of apocrine morphology with predicted response to anticancer therapeutics.** Box plots comparing predicted drug response scores for standard chemotherapeutic agents and targeted therapies between apocrine-marked and apocrine-negative. Lower values reflect greater predicted sensitivity to the corresponding agent. P values were calculated using the Wilcoxon test.